

## Friction-Induced Energy-Loss Rainbows in Atom Surface Scattering

Jeremy M. Moix and Eli Pollak\*

*Chemical Physics Department, Weizmann Institute of Science, 76100 Rehovoth, Israel*

Salvador Miret-Artés

*Instituto de Física Fundamental, Consejo Superior de Investigaciones Científicas, Serrano 123, 28006 Madrid, Spain*

(Received 15 October 2009; published 18 March 2010)

The rainbow is due to extrema of the angular deflection function of light impinging on water drops. Generically, extrema of suitably defined deflection functions lead to rainbows. These include angular and rotational rainbows in surface scattering and more. Here we introduce the concept of an “energy-loss deflection function” for scattering of particles from a periodic surface whose extrema lead to a new form—the “energy-loss rainbow” which appears as multiple maxima in the final energy distribution of the scattered particle. Energy-loss rainbows are caused by frictional phonon effects which induce structure in the energy-loss distribution instead of “washing it out.” We provide evidence that they have been observed in Ne scattering on self-assembled monolayers.

DOI: [10.1103/PhysRevLett.104.116103](https://doi.org/10.1103/PhysRevLett.104.116103)

PACS numbers: 68.49.Bc, 34.35.+a, 34.50.-s, 68.49.Df

One of the fascinating scenes provided by nature is the rainbow, whose rich history is summarized in Wikipedia [1]. A parallel ray of light hitting a spherical water droplet is refracted upon penetration of the droplet, then specularly reflected from the “back” of the droplet and then refracted upon exiting the droplet. The exit angle is a function of the impact parameter of the incident light and has an extremum at an angle of  $\sim 42^\circ$ , leading to the bright colors of the rainbow.

This effect also occurs when light is reflected from a periodically corrugated surface [2]. The specular reflection angle changes due to the corrugation. The exit angle as a function of the horizontal coordinate  $x$  will have at least two extrema leading to maxima in the angular distribution. Their separation increases with the corrugation amplitude [3]. The same happens when heavy atoms scatter from a periodically corrugated surface [2,4]. Experiments show (for a detailed list see Ref. [4]) that the angular distribution is at least doubly peaked [5,6]. Interaction of the scattered particle with the surface phonons causes the peaks to broaden and even merge into a single peak. Very recently, supernumerary rainbows have been measured in grazing collisions of fast atoms with a LiF(001) surface [7].

The term “rainbow scattering” has been generalized to include any scattering phenomenon in which the measured final property has an extremum with respect to an initial variable, leading to divergences in the distribution of the measured property. A well-known example is rotational rainbows. The final rotational angular momentum of a molecule colliding with a surface is a function of the initial orientation. Extrema of the “rotational deflection function” show up as experimentally measured maxima in the final rotational distribution [8,9]. The same phenomenon exists in principle for vibrations [10]. Rainbows are also well known in nuclear physics, where one considers

Coulomb and nuclear rainbows for the scattering of nuclei [11]. The rainbow effect occurs in ion channeling through thin crystals [12] and nanotubes [13] and in convoy electron scattering near surfaces [14].

In this Letter we report a new kind of rainbow, which we term the “energy-loss rainbow.” Consider the scattering of an atom from a periodic surface with incident energy  $E_i$  and incident angle  $\theta_i$  with respect to the surface normal. It is scattered with final energy  $E_f$  which typically will be lower than  $E_i$  due to energy loss to the surface via interaction with surface phonons. If the surface is corrugated, the final energy will be a function of the impact parameter. One may expect that the “energy deflection function” will have extrema which show up as divergences in the final energy distribution. These peaks would be the experimental manifestation of energy-loss rainbows. The mechanism is based on the general observation that the energy loss must be periodic due to the periodicity of the surface. In this context it is interesting to note that bimodal energy-loss distributions have been measured for a Ne atom colliding with a Self Assembled Monolayer (SAM) of 1-decanethiol on Au(111) [15,16].

It is also of special interest to note the multiple peak structure observed in energy and angle resolved alkali ion scattering from surfaces at a fixed final azimuthal angle [17]. Tenner *et al.* found [17] that maxima in the differential cross sections could be due to zeroes of the Jacobian determinant relating the final energy and scattering angles to the initial energy and horizontal position of the incident ion. These measurements perhaps are also an example of energy-loss rainbows although there is not enough experimental data available for determining the integral energy-loss cross section.

Energy-loss rainbows are due to the frictional effect of the surface. One normally thinks of friction as leading to

the “washing out” of rainbow structures. Here we find that it induces structure in the energy-loss distribution. Just like angular rainbows, as the surface temperature increases, the fluctuations become strong and the multiple peak structure is washed out. Energy-loss rainbows are not due to multiple scattering events. They exist even when all trajectories have a single collision with the surface. They are due to the surface corrugation dependent energy loss of the scattered atom.

To derive a theory for energy-loss rainbows we assume for simplicity in-plane scattering. The vertical and horizontal coordinates of the incident atom (with mass  $M$ ) are denoted as  $z$  and  $x$ , with conjugate momenta  $p_z$  and  $p_x$ . Our model Hamiltonian is taken to have the generic form [18]:

$$H = \frac{p_x^2 + p_z^2}{2M} + \bar{V}(z) + \bar{V}'(z)h \sin\left(\frac{2\pi x}{l}\right) + \frac{1}{2} \sum_{j=1}^N \left[ p_{j_z}^2 + \omega_{j_z}^2 \left( x_{j_z} - \frac{c_{j_z} \sqrt{M}}{\omega_{j_z}} g(z) \right)^2 \right] + \frac{1}{2} \sum_{j=1}^N \left[ p_{j_x}^2 + \omega_{j_x}^2 \left( x_{j_x} - \frac{lc_{j_x} \sqrt{M}}{2\pi \omega_{j_x}^2} \sin\left(\frac{2\pi x}{l}\right) g(z) \right)^2 \right]. \quad (1)$$

The vertical potential  $\bar{V}(z)$  is taken to be a Morse potential  $\bar{V}(z) = V_0(1 - e^{-\alpha z})^2 - V_0$  with  $V_0$  the physisorbed well depth and  $\alpha$  the stiffness parameter. We assume a sinusoidal surface corrugation with period  $l$  (the lattice length) and amplitude  $h$ . The corrugation is weak ( $h/l \ll 1$ ), allowing for expansion of the vertical potential in terms of a fluctuation along the horizontal coordinate. This then leads to the coupling  $\bar{V}'(z)$  between the vertical and horizontal modes of the incident atom. The phonon baths are independent, characterized by mass weighted momenta, coordinates, frequencies and coupling coefficients  $p_{j_i}$ ,  $x_{j_i}$ ,  $\omega_{j_i}$ ,  $c_{j_i}$ ,  $j = 1, \dots, N$ ;  $i = x, z$ . The baths are coupled to the vertical motion through the coupling function  $g(z) = \exp(-3\alpha z)$ . The coupling of the horizontal motion is periodic with respect to the horizontal coordinate and reflects the translational invariance of the Hamiltonian. It is this periodicity which underlies the energy-loss rainbow effect.

The equations of motion for linearly coupled harmonic baths are generalized Langevin equations (GLE's) [19]. In the continuum limit one introduces the spectral densities  $J_i(\omega) = \frac{\pi}{2} \sum_{j=1}^N \frac{c_{j_i}^2}{\omega_{j_i}} \delta(\omega - \omega_{j_i})$ ,  $i = x, z$ , and associated friction functions  $\eta_i(t) = \frac{2}{\pi} \int_0^\infty d\omega \frac{J_i(\omega)}{\omega} \cos(\omega t)$ ,  $i = x, z$ . We chose the friction to be Ohmic:  $\eta_i(t) = 2\eta_i \delta(t)$ ,  $i = x, z$  where  $\delta(t)$  is the Dirac “delta” function. The resulting Langevin equations of motion, which are given explicitly in Ref. [18] were solved numerically.

For the generic Hamiltonian of Eq. (1) we have shown in Ref. [18] that in the limit of weak corrugation and weak friction, the energy-loss distribution has the form

$$P(E_f) = \frac{1}{l} \int_0^l dx \left( \frac{1}{4\pi k_B T \langle \Delta E(x) \rangle} \right)^{1/2} \times \exp\left( -\frac{(E_f - E_i + \langle \Delta E(x) \rangle)^2}{4k_B T \langle \Delta E(x) \rangle} \right), \quad (2)$$

where  $\langle \Delta E(x) \rangle$  is the energy-loss deflection function—it is the average energy lost to the surface at impact parameter  $x$ ,  $k_B$  is Boltzmann's constant and  $T$  is the surface temperature. This result generalizes Brako's result [20] for the energy loss, which was derived without considering surface corrugation. Its validity is rather general, the phonons must be considered as a linearly coupled harmonic bath and the energy loss must be translationally invariant. The energy deflection function depends linearly on the friction coefficient (in the weak damping limit) but is temperature independent since it gives the average change in the energy loss; the Gaussian fluctuations at any energy average out to zero. The effect of the fluctuations, and thus the temperature, is then to broaden the energy-loss distribution, as is also evident from Eq. (2).

As a *predictive* example we consider the scattering of Ar on LiF(100), studied recently by Kondo *et al.* [6], who measured the in-plane angular distribution as a function of incidence energy which varied from 315 to 705 meV at  $T = 300$  K. We fit their experimental data by numerically solving the Langevin equations of motion. The measured experimental angular distributions were fit quantitatively by adjusting the free parameters of the model. The resulting values were  $\alpha l = 5$ ,  $\alpha h = 0.05$ ,  $\eta_x/\omega_0 = 1.41 \times 10^{-4}$ , and  $\eta_z \alpha/\omega_0 = 1.13 \times 10^{-3}$ , where  $\omega_0 = \sqrt{2V_0 \alpha^2/M}$  is the harmonic frequency of the Morse potential. The physisorbed well depth  $V_0$  was taken to be 150 meV (somewhat larger than the 88 meV of Ref. [21]). The lattice length is [22]  $l = 4 \text{ \AA}$ .

At the low energies of the incident beam the analytic energy distribution calculated from Eq. (2) is in quantitative agreement with the numerical simulations. However, in this regime the energy-loss rainbows can be observed only at very low temperatures, so below we present results at a higher energy of 3000 meV which is well within the range of typical experimental capabilities. At this energy, the perturbative treatment used in deriving Eq. (2) begins to fail and a broader energy distribution is always predicted compared to the numerical results. We found that a simple scaling of the variance in Eq. (2) by the factor  $1 - a \cos(\theta_i)$  with  $a = 0.825$ , brings the analytical and numerical results into agreement for all angles and temperatures studied.

Using the parameters specified above, results for the energy-loss deflection function are shown in Fig. 1 at an incident energy of 3000 meV,  $T = 0$  K and for the angles of incidence of  $0^\circ$ ,  $15^\circ$ ,  $45^\circ$ , and  $60^\circ$ . Within the Langevin equation formalism, and weak coupling to the baths, the energy-loss deflection function is independent of temperature, since the Gaussian fluctuations induced by finite temperature average out to zero. This prediction was verified in our simulations. The energy loss to the bath can lead

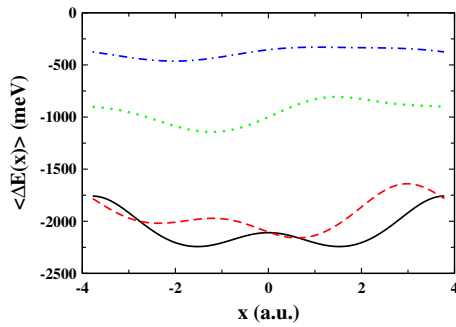


FIG. 1 (color online).  $T = 0$  K theoretical computation of the energy loss to the bath as a function of the impact parameter for the scattering of Ar from a LiF(100) surface. The solid (black), dashed (red), dotted (green) and dot-dashed (blue) lines correspond to incident angles of  $0^\circ$ ,  $15^\circ$ ,  $45^\circ$ , and  $60^\circ$ , respectively. Note the multiple extrema of the “energy-loss deflection functions”.

to a rich structure in the corresponding energy distribution. As can be seen from the extrema of the deflection functions, four peaks are expected at a scattering angle of  $15^\circ$ , and two rainbow energies are anticipated at  $60^\circ$  as borne out in the low temperature energy distributions presented below.

We computed the resulting energy-loss distributions in two different ways. The solid lines in Fig. 2 are obtained by inserting the numerically determined energy-loss deflection functions into the modified form of Eq. (2). The symbols show the distributions obtained directly from the simulations. Panels (a)–(d) show the integral energy-loss distributions (integrated over all final scattering angles) for the scattering of Ar on the LiF(100) surface calculated at the incidence angles  $0^\circ$ ,  $15^\circ$ ,  $45^\circ$ , and  $60^\circ$ , respectively, and at  $T = 0.5, 30,$  and  $90$  K. As the surface temperature and incident angle increase, the rainbow structure is broad-

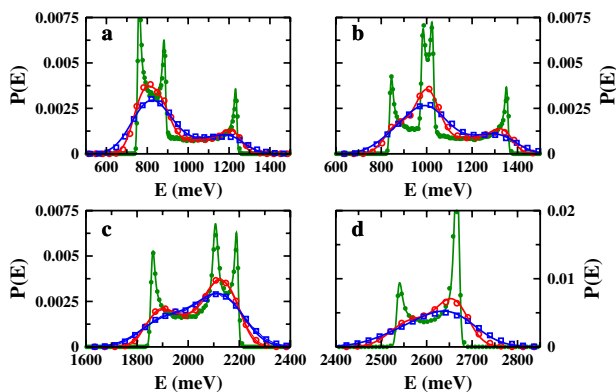


FIG. 2 (color online). Theoretical final energy distributions of Ar scattered on a LiF(100) surface at incidence angles of  $0^\circ$ ,  $15^\circ$ ,  $45^\circ$ , and  $60^\circ$  displayed in panels (a)–(d). The (green) dots, (red) circles, and (blue) squares correspond to the numerical distributions calculated at  $T = 0.5, 30,$  and  $90$  K, respectively. The solid lines show the analytic distributions calculated from Eq. (2) using the modified form of the variance.

ened and eventually disappears, as seen particularly in the case of  $60^\circ$ . It is notable that at the lowest temperature the energy rainbows show the divergence which is characteristic of angular rainbows.

Since it is easier to measure the energy loss at a fixed final scattering angle we consider in Fig. 3 the joint distribution for the  $T = 30$  K results shown in panel (b) of Fig. 2. These typical results show that one should expect a double peak energy-loss distribution for most angles. They also show that the energy-loss rainbows are not necessarily related to the angular rainbows. They can come from a different region of the surface.

We have thus demonstrated through numerical simulation that there exist in principle energy-loss rainbows. The condition for their observation is that the distance between the energy-loss rainbows  $\Delta E_R$  is larger than the variance of the energy distribution  $\sim \sqrt{2k_B T \langle \Delta E \rangle}$  (where  $\langle \Delta E \rangle$  is the overall average energy loss). This condition implies three ways for increasing the chance for observation of the energy-loss rainbows. They are (a) lowering the surface temperature and (b) increasing the incidence energy. The distance between the energy-loss rainbows increases linearly with increasing incidence energy while the width increases only as the square root of the energy loss. (c) Changing the angle of incidence which may also lead to an increase in the spacing between energy-loss peaks.

Have energy-loss rainbows actually been observed experimentally? Sibener and co-workers measured the energy-loss distribution of Ne scattered from a SAM of 1-decanethiol on Au(111) [15,16]. They observed a bimodal distribution for a  $45^\circ$  angle of incidence and Ne incident energies of 250 and 550 meV which disappeared when the angle of incidence was increased to  $60^\circ$  and the energy lowered to 65.3 meV. At 250 (550) meV the distance between the peaks is  $\sim 120$  ( $\sim 270$ ) meV. In contrast to atom scattering off liquids (where bimodal distributions have been observed [23]), the low energy peak observed in Ref. [16] is not a thermal trapping-desorption peak [16,24].

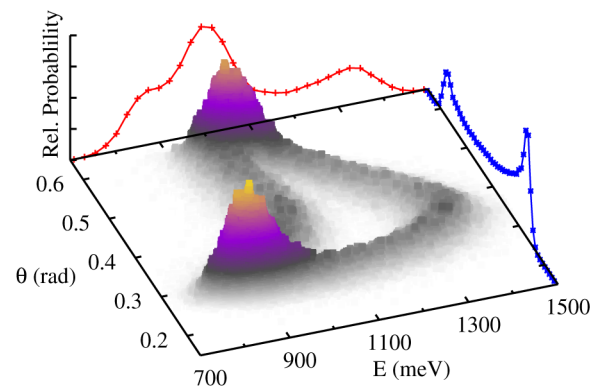


FIG. 3 (color online). Theoretical joint energy loss and angular distribution for Ar scattered from LiF at  $T = 30$  K and incident energy of 3 eV. Also shown are the integrated angular and energy-loss distributions. Note the relation between the angular rainbows and the energy-loss rainbows.

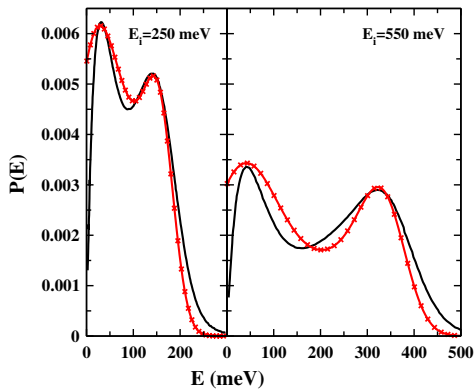


FIG. 4 (color online). Comparison of theoretical (crossed lines) and experimental [16] (solid lines) energy-loss distributions for the scattering of Ne from a SAM of 1-decanethiol on Au(111).

Isa *et al.* [16] attribute the bimodal peak to Ne colliding with different parts of the adsorbed molecule at different lateral distances. It is precisely the different lateral distances which give rise to the energy-loss rainbows in our theory. Using the theoretical expression for the energy loss [Eq. (2)] with the same functional form used to fit the numerical data in Fig. 1:  $\Delta E(x) = 0.0147 - 0.0065 \cos(2\pi x) - 0.00175 \cos(4\pi x) + 0.0009 \cos(6\pi x)$  a.u. for  $E = 550$  meV and  $\Delta E(x) = (0.01475 - 0.0065 \cos(2\pi x) - 0.002 \cos(4\pi x) + 0.00055 \cos(6\pi x))250/550$  a.u. for  $E = 250$  meV, we show in Fig. 4 a comparison between the fitted theoretical energy-loss distribution for directly scattered particles with the measured experimental energy-loss distributions. The good agreement (better than obtained in the numerical simulations of Ref. [16]) indicates that the peaks reflect the energy-loss rainbows. Our theory also predicts that increasing the angle of incidence and lowering the energy will wash out the rainbow features, as observed in Fig. 8 of Ref. [16].

In summary, we presented a general theory for energy-loss rainbows which are due to phonon induced friction. They have been confirmed through our numerical simulations and perhaps also experimentally in measurements of Ne scattering from a SAM and  $K^+$  ions scattering from W(110) [17]. The present theory predicts that the energy-loss rainbows will be observed for the scattering of Ar from the LiF(100) surface. Lowering the temperature, changing the angle of incidence and raising the incident energy should ultimately lead to at least a bimodal energy-loss distribution also for this system.

This work was supported by grants from the Israel Science Foundation, the Albert Einstein Minerva Center at the Weizmann Institute of Science, and the Ministry of Science and Innovation of Spain through project FIS2007-62006.

\*eli.pollak@weizmann.ac.il

- [1] <http://en.wikipedia.org/wiki/Rainbow>.
- [2] J. D. McClure, J. Chem. Phys. **51**, 1687 (1969); **52**, 2712 (1970); **57**, 2810 (1972).
- [3] W. A. Steele, Surf. Sci. **38**, 1 (1973).
- [4] A. W. Kleyn and T. C. M. Horn, Phys. Rep. **199**, 191 (1991).
- [5] J. N. Smith, D. R. O'Keefe, and R. L. Palmer, J. Chem. Phys. **52**, 315 (1970); E. Hulpke, Surf. Sci. **52**, 615 (1975); E. Hulpke and K. Mann, Surf. Sci. **133**, 171 (1983); **157**, 245 (1985); T. Engel and J. H. Weare, Surf. Sci. **164**, 403 (1985); K. H. Rieder and W. Stocker, Phys. Rev. B **31**, 3392 (1985); A. Amirav, M. J. Cardillo, P. L. Trevor, C. Lim, and J. C. Tully, J. Chem. Phys. **87**, 1796 (1987).
- [6] T. Kondo, H. S. Kato, T. Yamada, S. Yamamoto, and M. Kawai, Eur. Phys. J. D **38**, 129 (2006).
- [7] A. Schüller and H. Winter, Phys. Rev. Lett. **100**, 097602 (2008).
- [8] A. W. Kleyn, A. C. Luntz, and D. J. Auerbach, Phys. Rev. Lett. **47**, 1169 (1981); R. Schinke, J. Chem. Phys. **76**, 2352 (1982); J. A. Barker, A. W. Kleyn, and D. J. Auerbach, Chem. Phys. Lett. **97**, 9 (1983).
- [9] D. Beck, in *Physics of Electronic and Atomic Collisions*, edited by S. Datz (North Holland, Amsterdam, 1982), p. 331; M. Faubel, Adv. At. Mol. Phys. **19**, 345 (1983); U. Buck, Comments At. Mol. Phys. **17**, 143 (1986).
- [10] G. Drolshagen, H. R. Mayne, and J. P. Toennies, J. Chem. Phys. **75**, 196 (1981); R. De Jonge, J. Los, and A. E. de Vries, Nucl. Instrum. Methods Phys. Res., Sect. B **30**, 159 (1988); P. J. Van den Hoek and A. W. Kleyn, J. Chem. Phys. **91**, 4318 (1989).
- [11] M. E. Brandan and G. R. Satchler, Phys. Rep. **285**, 143 (1997).
- [12] N. Nesković, Phys. Rev. B **33**, 6030 (1986).
- [13] S. Petrović, D. Borka, and N. Nesković, Adv. Studies Theor. Phys. **2**, 415 (2008).
- [14] G. Ziegler, M. Rädle, O. Pütz, K. Jung, H. Ehrhardt, and K. Bergmann, Phys. Rev. Lett. **58**, 2642 (1987).
- [15] T. Yan, N. Isa, K. D. Gibson, S. J. Sibener, and W. L. Hase, J. Phys. Chem. A **107**, 10600 (2003).
- [16] N. Isa, K. D. Gibson, T. Yan, W. L. Hase, and S. J. Sibener, J. Chem. Phys. **120**, 2417 (2004).
- [17] A. D. Tenner, K. T. Gillen, T. C. M. Horn, J. Los, and A. W. Kleyn, Phys. Rev. Lett. **52**, 2183 (1984); A. D. Tenner, R. P. Saxon, K. T. Gillen, D. E. Harrison, Jr., T. C. M. Horn, and A. W. Kleyn, Surf. Sci. **172**, 121 (1986).
- [18] E. Pollak and S. Miret-Artés, J. Chem. Phys. **130**, 194710 (2009).
- [19] R. Zwanzig, J. Stat. Phys. **9**, 215 (1973).
- [20] R. Brako and D. M. Newns, Phys. Rev. Lett. **48**, 1859 (1982); R. Brako, Surf. Sci. **123**, 439 (1982).
- [21] J. R. Klein and M. W. Cole, Surf. Sci. Lett. **81**, L319 (1979).
- [22] Y. Ekinici and J. P. Toennies, Surf. Sci. **563**, 127 (2004).
- [23] M. E. King, M. E. Saecker, and G. M. Nathanson, J. Chem. Phys. **101**, 2539 (1994).
- [24] T. Yan, W. L. Hase, and J. R. Barker, Chem. Phys. Lett. **329**, 84 (2000).